

An Unequal Error Protection Scheme for JPEG Image Transmission Using Enhanced Duo-Binary Turbo Codes

Tulsi Pawan Fowdur

Dept of Electrical and Electronic Engineering
University of Mauritius
Reduit, Mauritius
e-mail: p.fowdur@uom.ac.mu

Yashvin Beni

Dept of Electrical and Electronic Engineering
University of Mauritius
Reduit, Mauritius
e-mail: yashvinbeni@gmail.com

Abstract— JPEG is a widely deployed image compression standard used in several applications. However, JPEG image transmission is challenging and sophisticated strategies are required for reliable transmission. This paper investigates the performance of JPEG image transmission using duo-binary Turbo codes with Unequal Error Protection (UEP). UEP is achieved by applying a lower code-rate to protect the DC-layer of the image more efficiently and a higher code-rate for protecting the AC-layer. Additionally, the duo-binary Turbo code is enhanced by scaling its extrinsic information to improve performance and by using a stopping criterion to limit the number of iterations required for decoding. The proposed UEP scheme provides a gain of at least 10 dB in Peak Signal to Noise Ratio (PSNR) over an Equal Error Protection (EEP) scheme for a range of E_b/N_0 values. Moreover, the gain in PSNR increases as the couple length of the duo-binary code is increased.

Keywords- JPEG; UEP; Duo-Binary Turbo Codes.

I. INTRODUCTION

JPEG is a Discrete Cosine Transform (DCT) based image compression algorithm, which employs Huffman coding to generate a compressed bit-stream [1]. It is a widely adopted standard and forms an integral part of several applications such as web browsing and telemedicine [2]. However, the use of Huffman coding renders the JPEG coded bit-stream very sensitive to error propagation because a single bit in error can cause a complete loss of synchronisation. As such, sophisticated coding solutions are required to ensure reliable transmission. One solution is to use powerful error-correcting codes such as Turbo codes, which are well suited to protect image data as recently demonstrated in [3]. Error resilient and concealment techniques also provide a significant improvement in transmission fidelity [4,5]. Moreover, a highly efficient strategy for achieving robust JPEG image transmission is UEP. UEP consists of exploiting the fact that the DCT operation in JPEG, segments the image into layers of unequal importance. Hence, by allocating different levels of protection to these layers, a significant gain in the overall quality of the received image can be obtained.

Several efficient UEP schemes have been developed for JPEG image transmission using Turbo codes. For example, in [6], UEP and joint source channel decoding with a-priori statistics were combined and applied to JPEG image transmission. Both Turbo codes and Turbo and Turbo Trellis Coded Modulation were used and major gains in PSNR were obtained over conventional JPEG image transmission schemes. An error resilient wireless JPEG image transmission scheme, which employed product Turbo or Reed Solomon codes alongside an optimal UEP algorithm was proposed in [7]. Moreover, in [8], an UEP scheme, which employs s-random odd-even interleaving with odd-even puncturing, as well as a new UEP scheme for the soft output Viterbi algorithm, were proposed. Improved BER and PSNR performances in JPEG image transmission were obtained with these UEP schemes [8]. Finally, in [9], the performance of three UEP schemes for progressive JPEG image transmission using delay-constrained hybrid ARQ, with iterative bit and symbol combining was proposed. Gains of over 9 dB in PSNR were obtained with the UEP schemes as compared to their corresponding Equal Error Protection (EEP) schemes.

In contrast with previous works, which considered binary Turbo codes, this paper proposes an UEP scheme based on duo-binary Turbo codes. These codes provide better convergence of iterative decoding, have reduced latency, lower sensitivity to puncturing, larger minimum distance and lower memory requirement [10]. Also, the duo-binary code is modified with a scale factor [11,12] and stopping criterion [13] to further improve the performance of the UEP scheme. The proposed UEP scheme allocates more protection to the DC layer, which contains the most significant part of the image after the DCT operation, and less protection to the AC layer. This is achieved by using the puncturing matrices specified for the duo-binary Turbo code of the DVB-RCS standard [14]. The UEP scheme outperforms the EEP scheme by at least 10 dB in PSNR over a range of E_b/N_0 values. Moreover, the gain in PSNR increases as the couple length of the duo-binary code is increased.

The organization of this paper is as follows. Section II describes the complete system model. Section III presents the simulation results and analysis. Section IV concludes the paper.

II. SYSTEM MODEL

The complete encoding process is shown in Figure 1. The input image is fed to the JPEG encoder, which operates on blocks of 8x8 pixels and performs DCT, quantization and zig-zag ordering [1]. The AC and DC coefficients are then separated into the AC and DC layers. The DC layer regroups the first coefficient from all 8x8 blocks obtained after zig-zag ordering and the AC-layer is the concatenation of the 63 coefficients from all 8x8 blocks. For example with a 256x256 image, there are 1024 blocks of size 8x8 and each block has one DC coefficient and 63 AC coefficients. The DC layer hence contains 1024 coefficients and the AC layer contains 1024x63 coefficients. To prevent error propagation, the AC and DC layers are divided into blocks of 63 and 64 coefficients respectively. The blocks of the DC layer undergo Differential Pulse Code Modulation (DPCM) and DC-Huffman coding. Each block is encoded separately and after Huffman coding a header is inserted to indicate the size in bits of the resulting DC-packet. The blocks of the AC-layer undergo Run-Length Encoding (RLE) followed by AC-Huffman coding and a header is appended to indicate the size of each AC-packet. Each DC and AC packet can be decoded independently and errors within a packet do not propagate throughout the DC or AC layer.

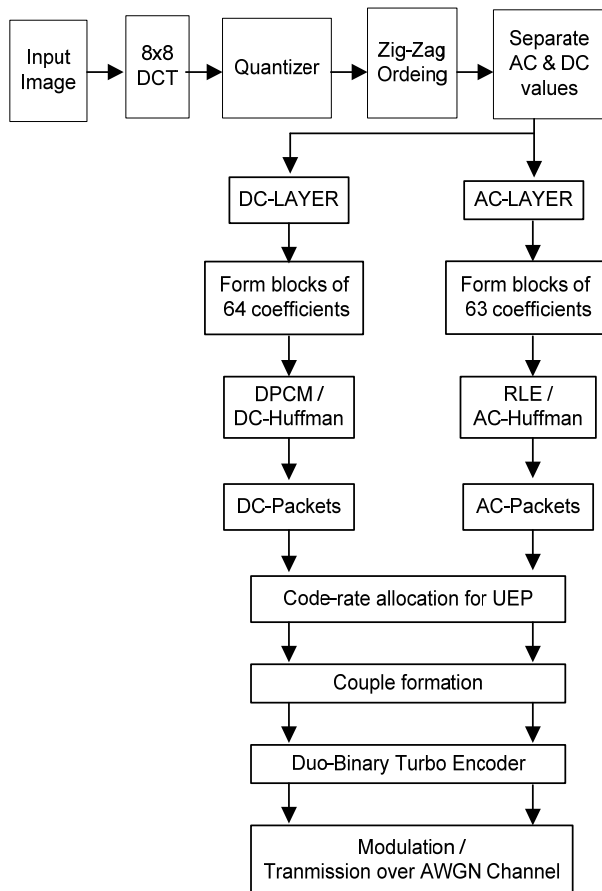


Figure 1. Complete encoding system with UEP.

A code-rate allocation is performed to provide UEP to the DC and AC packets. The DC packets are given the lowest code-rate while the AC-packets are allocated a higher code-rate. The packets are then converted into couples of length N before being sent to the duo-binary Turbo encoder. The headers are transmitted error-free through a side-channel. Finally, the encoded couples are QPSK modulated and sent over an Additive White Gaussian Noise (AWGN) channel.

The decoding system is shown in Figure 2. The received noisy array, R_t is de-punctured as appropriate and sent to the first duo-binary decoder, DEC1. DEC2 receives the interleaved counterpart of R_t . The decoders employ the Max-Log-MAP algorithm to compute the following parameters:

(a) $\overline{\gamma}_t^{q(i)}(l', l)$: The branch transition probability from state l' to l of symbol i at time instant t where $i \in \{0,1,2,3\}$ for decoder q , where $q = 1$ or 2 . It is computed as follows for the first decoder.

$$\overline{\gamma}_t^{1(i)}(l', l) = \log \left[p(u_t^2 = i) \cdot \exp \left(- \frac{[R_t - x_t^i(l)]^2}{2\sigma^2} \right) \right] \tag{1}$$

$$= \log [p(u_t^2 = i)] - \left(\frac{[R_t - x_t^i(l)]^2}{2\sigma^2} \right)$$

where,

$p(u_t^2 = i)$ is the a-priori probability of symbol i obtained from the second decoder,

$x_t^i(l)$ is the modulated complex symbol at time t , associated with the transition from state $S_{t-1} = l'$ to $S_t = l$ and input symbol i ,

$R_t(l)$ is the received systematic and parity complex symbols at time t .

For the second decoder, the computation of $\overline{\gamma}_t^{2(i)}(l', l)$ is similar to equation (1) except that it uses the interleaved version of the systematic symbols of R_t , a different set of complex parity symbols and the a-priori probability of symbol i obtained from the first decoder i.e., $p(u_t^1 = i)$.

(b) $\overline{\alpha}_t^q(l)$: The forward recursive variable at time t and state l . It is computed according to the following equation for a decoder with M_s states:

$$\overline{\alpha}_t^q(l) = \log \sum_{l'=0}^{M_s-1} e^{\overline{\alpha}_{t-1}^{q(l')} + \overline{\gamma}_t^{q(i)}(l', l)} \tag{2}$$

(c) $\overline{\beta}_t^q(l)$, which is the backward recursive computed at time t as follows:

$$\overline{\beta}_t^q(l) = \log \sum_{l'=0}^{Ms-1} e^{\overline{\beta}_{t+1}^q(l') + \gamma_{t+1}^q(l,l')} \quad (3)$$

(d) $\Lambda_{q(i)}(t)$, which is the Log Likelihood Ratio (LLR) of symbol i where $i \in (1,2,3)$, and the LLRs are normalized to the symbol '0'. This parameter is computed as follows:

$$\Lambda_{q(i)}(t) = \log \left[\frac{\sum_{l'=0}^{Ms-1} e^{\alpha_{t-1}^q(l') + \gamma_t^q(l',l) + \overline{\beta}_t^q(l)}}{\sum_{l'=0}^{Ms-1} e^{\alpha_{t-1}^q(l') + \gamma_t^q(l',l) + \overline{\beta}_t^q(l)}} \right] \quad (4)$$

(e) $\Lambda_{1es(i)}(t)$ and $\Lambda_{2es(i)}(t)$: The extrinsic information of symbol i where $i \in (1,2,3)$, are generated by DEC1 and DEC2 respectively. They are computed as follows:

$$\Lambda_{1es(i)}(t) = \Lambda_{1(i)}(t) - \overline{\Lambda}_{2es(i)}(t) - \Lambda_{1in(i)}(t) \quad (5)$$

$$\Lambda_{2es(i)}(t) = \Lambda_{2(i)}(t) - \overline{\Lambda}_{1es(i)}(t) - \Lambda_{2in(i)}(t) \quad (6)$$

$\Lambda_{1in(i)}(t)$ and $\Lambda_{2in(i)}(t)$ are the intrinsic information of symbol i where $i \in (1,2,3)$, are generated by DEC1 and DEC2 respectively.

Further details on the computation of these parameters are given in [14,15,16]. In the enhanced Duo-binary decoder, the extrinsic information produced by both decoders are multiplied by a scale factor S as shown in Figure 2. The application of the scale factor improves performance because the extrinsic information value output by the Turbo decoder is most of the time too optimistic, hence by scaling it, better performance is achieved [11-12]. The controller unit accepts the extrinsic information from both decoders and uses a stopping criterion [13] to stop the iterative decoding process. At the start of the iterative decoding process, switches $S1$ and $S2$ are ON and when a given condition is met, the controller unit turns OFF both switches to stop the iterative decoding process. In this way, the decoder avoids the use of extra iterations and reduces the decoding complexity. This technique also reduces the power consumption of the decoder.

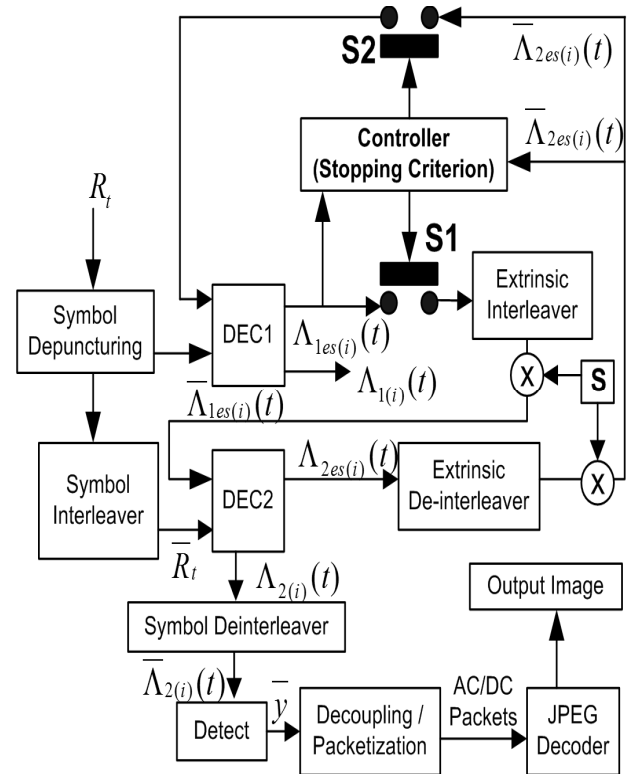


Figure 2. Decoding system with enhanced duo-binary Decoder.

A detailed algorithm for the decoding process is now presented. In this algorithm, steps 4-12 correspond to the operations of DEC1 and steps 13-21 of DEC2. The parameters $M_{11}^r(t), M_{12}^r(t), M_{21}^r(t), M_{22}^r(t)$ are used in the stopping criterion and the function $f(\cdot)$ counts the number of sign changes between the two arguments that are passed to it. The function $detect(\cdot)$ determines the maximum of the LLR values and outputs either symbol 0,1,2 or 3. The variable j increases by 1 because the decoder processes one couple at a time up to a maximum of N_c , which is the total number of couples in the image. The variable r also increases by 1 up to a maximum limit of r_{max} . However, the variable $num_iterations$, which is used to count the number of iterations consumed by the decoder, is incremented by 0.5. This is because the stopping criterion can stop the decoding process after either DEC1 or DEC2 whereby each decoder consumes 0.5 iterations. For example, if for a given couple, the decoding process completes 2 full iterations and then at the third iteration i.e., $r=3$, after passing through DEC1, the stopping criterion is satisfied, then only 0.5 additional iteration is consumed and hence $num_iterations$ will be 2.5 and not 3. The complete decoding algorithm is as follows:

1. num_iterations = 0
2. for j = 1:N_c
3. for r = 1:r_{max}
4. Compute: $\overline{\gamma}_t^{(i)}(l', l), \overline{\alpha}_t^1(l), \overline{\beta}_t^1(l), \Lambda_{1es(i)}(t), \Lambda_{1(i)}(t)$
5. num_iterations = num_iterations + 0.5.
6. $M_{11}^r(t) = \max(\Lambda_{1es(2)}(t), \Lambda_{1es(3)}(t)) - \max(\Lambda_{1es(0)}(t), \Lambda_{1es(1)}(t))$
7. $M_{12}^r(t) = \max(\Lambda_{1es(1)}(t), \Lambda_{1es(3)}(t)) - \max(\Lambda_{1es(0)}(t), \Lambda_{1es(2)}(t))$
8. if (r>1)
9. if ($f(M_{11}^r(t), M_{11}^{r-1}(t)) \leq \frac{1}{N}$ or $f(M_{12}^r(t), M_{12}^{r-1}(t)) \leq \frac{1}{N}$)
10. Goto: line 23
11. endif
12. endif
13. Compute: $\overline{\gamma}_t^{(i)}(l', l), \overline{\alpha}_t^2(l), \overline{\beta}_t^2(l), \Lambda_{2es(i)}(t), \Lambda_{2(i)}(t)$
14. num_iterations = num_iterations + 0.5.
15. $M_{21}^r(t) = \max(\Lambda_{2es(2)}(t), \Lambda_{2es(3)}(t)) - \max(\Lambda_{2es(0)}(t), \Lambda_{2es(1)}(t))$
16. $M_{22}^r(t) = \max(\Lambda_{2es(1)}(t), \Lambda_{2es(3)}(t)) - \max(\Lambda_{2es(0)}(t), \Lambda_{2es(2)}(t))$
17. if (r>1)
18. if ($f(M_{21}^r(t), M_{21}^{r-1}(t)) \leq \frac{1}{N}$ or $f(M_{22}^r(t), M_{22}^{r-1}(t)) \leq \frac{1}{N}$)
19. Goto: line 23
20. endif
21. endif
22. Endfor
23. Decoded couple, $\overline{y} = \text{detect}(\overline{\Lambda}_{2(i)}(t))$
24. Endfor
25. Convert the received couples into AC and DC packets.
26. Perform JPEG decoding on the received packets.

III. SIMULATION RESULTS AND ANALYSIS

The performances of the following four schemes for JPEG image transmission are compared:

Scheme 1- UEP with scale factor: This scheme employs UEP to provide different levels of protection to the AC and

DC packets of the image. It also uses a scale factor, S, to enhance the performance of the duo-binary Turbo code by scaling the extrinsic information, as depicted in Fig.2. The value of S has been set to 0.75 in this simulation.

Scheme 2 - UEP without scale factor: This scheme is similarly to Scheme 1 but the extrinsic information is not scaled and the value of S is set to 1.0 in Fig.2.

Scheme 3 - EEP with scale factor: It is similar to Scheme 1 but equal protection is given to the AC and DC packets.

Scheme 4 - EEP without scale factor: This scheme is similar to Scheme 3 but the scale factor, S, is set to 1.0.

In all simulations, the DVB-RCS standard duo-binary Turbo code [14] has been used with a stopping criterion. The generator polynomials in octal are g1 = 15 for the feedback branch, g2 = 13 and g3 = 11 for the parity branches. Couple lengths of N=64 and N=212 are used and the maximum number of iterations, r_{max} = 12. Puncturing matrices are chosen as per the DVB-RCS standard and the 256x256 Lena image is used as input. Moreover, it is assumed that the headers are transmitted error free over a strongly protected side channel.

The overall coding rate, O_c, was limited to O_c < 0.97 bits/pixel and to ensure a fair comparison the overall coding rate for UEP was kept below that of EEP. However, with UEP the DC couples are more strongly protected with a code-rate of 1/3 while the AC couples are allocated a code-rate of 4/5. On the other hand the EEP schemes allocates a fixed code-rate of 2/3 to both DC and AC couples. The overall coding rate, O_c, is computed as follows:

$$O_c = \frac{1}{T} \left(\frac{T_{DC}}{R_{DC}} + \frac{T_{AC}}{R_{AC}} \right) \quad (7)$$

where,

T is total number of pixels in the image,
T_{DC} is the total number of bits in the DC couples,
R_{DC} is the code-rate allocated to the DC couples,
T_{AC} is the total number of bits in the DC couples,
R_{AC} is the code-rate allocated to the DC couples.

The source coding rate, S_c, and O_c, vary with the couple length because different numbers of padding bits are required to convert the bit stream from the JPEG encoder into couples of length N.

Table I gives the values of O_c and S_c for different couple lengths, N.

TABLE I
CODING RATES FOR DIFFERENT VALUES OF N

N	T _{DC}	T _{AC}	S _c	O _c	
				UEP	EEP
64	5760	36096	0.639	0.952	0.958
212	5936	36040	0.641	0.959	0.961

Figure 3 shows the graph of PSNR versus Eb/No for the four schemes with N = 64. The UEP scheme with scale factor provides a gain of 7dB in PSNR over the EEP schemes at Eb/No = 1.5dB and a major gain of 12dB in PSNR in the range 2dB ≤ Eb/No ≤ 3dB. It also outperforms the UEP scheme without scale factor by 1dB in PSNR in the range 2dB ≤ Eb/No ≤ 3dB. This gain is achieved because with the UEP the DC layer is recovered with fewer errors than the AC-layer and hence, the image can be reconstructed with much less distortions. However, it is observed that at high Eb/No values, the gain obtained with UEP over EEP decreases because the overall errors introduced in the image is considerably less.

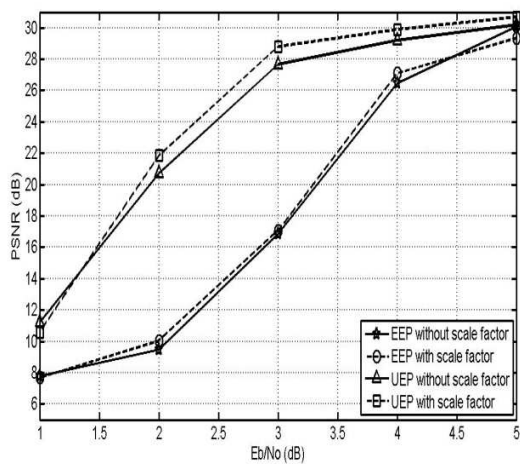


Figure 3. Graph of PSNR against Eb/No for N = 64.

The graph of number of iterations versus Eb/No for N = 64 is shown in Figure 4. The stopping criterion allows the number of iterations and hence the decoding complexity to decrease progressively as the Eb/No is increased. Interestingly, the UEP scheme with scale factor requires less iterations than the EEP schemes in the range 1dB ≤ Eb/No ≤ 3dB and provides an impressive reduction of 5.5 iterations over the EEP scheme without scale factor at Eb/No = 1dB.

Figure 5 shows the graph of PSNR versus Eb/No for the four schemes with N = 212. The UEP scheme with scale factor provides a gain of 10dB in PSNR over the EEP schemes at Eb/No = 1dB and a major gain of 15 dB in PSNR in the range 1.5 dB ≤ Eb/No ≤ 2dB. It also outperforms the UEP scheme without scale factor by about 1dB in PSNR in the range 1dB ≤ Eb/No ≤ 2dB. Moreover, with N = 212 the UEP scheme with scale factor outperforms the UEP scheme with scale factor for N = 64, by an average of 5 dB in PSNR. The gain is greater with a couple length of N=212 because the performance of the duo-binary Turbo code improves with increase in couple length.

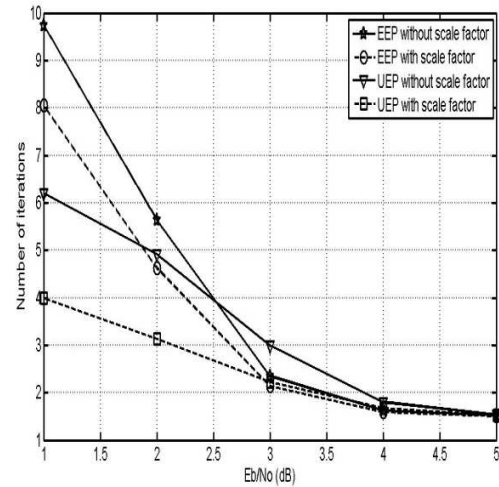


Figure 4. Number of iterations against Eb/No for N = 64.

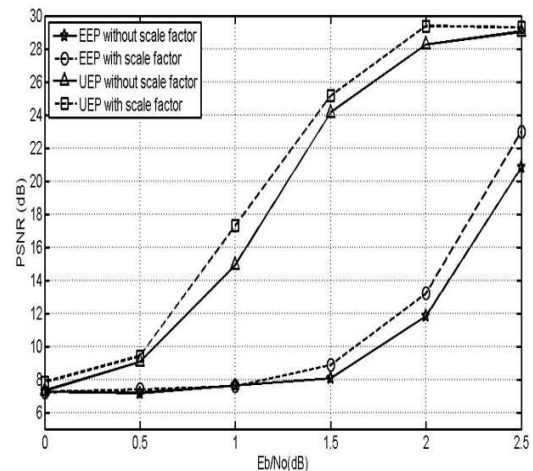


Figure 5. Graph of PSNR against Eb/No for N = 212.

The graph of number of iterations versus Eb/No for N = 212 is shown in Figure 6. It is observed that when N=212, the UEP scheme with scale factor takes less iterations than the EEP schemes only in the range 0dB ≤ Eb/No ≤ 1dB. For Eb/No > 1.5 dB the EEP scheme with scale factor requires significantly less iterations than the UEP schemes, for example, at Eb/No = 2.5dB it requires 5 iterations less than the UEP scheme without scale factor. A possible explanation for that is that the threshold used in the stopping criterion was not optimized for N = 212 and was maintained at 1/N.

There are two ways in which the UEP scheme can lead to an increase in complexity with respect to the EEP scheme. Firstly, over a certain Eb/No range, as observed in Figure 5, the UEP scheme requires more iterations than the EEP scheme. Secondly, with the UEP scheme, the duo-binary

Turbo encoder must treat the AC and DC packets separately and use different code-rates, hence different puncturing patterns are required for each of them. The same applies for the duo-binary Turbo decoder, whereby a different de-puncturing process must be used for the AC and DC packets.

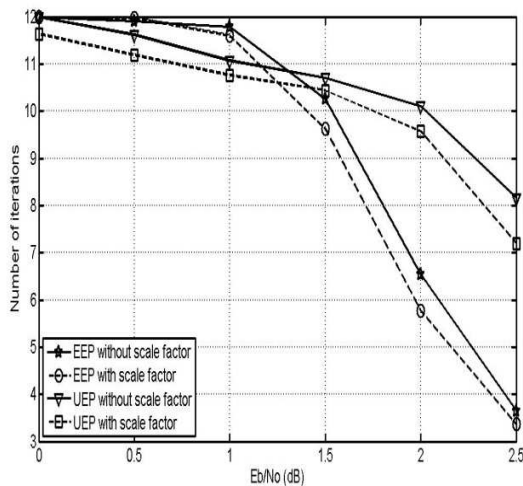


Figure 6. Number of iterations against Eb/No for N = 212.

IV. CONCLUSION

This paper proposed an efficient UEP scheme for JPEG image transmission with enhanced duo-binary Turbo codes whereby an extrinsic scale factor and stopping criterion were incorporated. The performances of four schemes were compared with couple lengths of 64 and 212. The results showed that major gains of the order of 10 dB in PSNR are obtained with the UEP scheme over conventional EEP schemes and this gain increases when the couple length is increased from 64 to 212. Furthermore, the use of the scale factor improved the PSNR performance and reduced the number of iterations required, hence the complexity. Interestingly, with a couple length of 64, the UEP scheme required fewer iterations than the EEP schemes. However, with a couple length of 212, at higher Eb/No values, the EEP schemes required less iterations. An interesting future work would be to optimize the threshold used in the stopping criterion for couple lengths greater than 64, so as to reduce the number of iterations required by the UEP schemes.

ACKNOWLEDGMENT

The authors would like to thank the University of Mauritius for providing the necessary facilities for conducting this research and the reviewers for their valuable comments.

REFERENCES

- [1] R.C. Gonzalez, R.E Woods, and S.L Eddins, Digital Image Processing in Matlab, 2nd ed., Gatesmark Publishing, (2009).
- [2] L.G. Yamamoto, "Using JPEG image transmission to facilitate telemedicine," The American Journal of Medicine, vol. 13, pp. 55-57, 2009.
- [3] Ersin GOSE, "Adaptive Wiener-turbo systems with JPEG & bit plane compressions in image transmission," Turk J Elec Eng & Comp Sci, vol. 19, no.1, 2011. (doi:10.3906/elk-1003-461).
- [4] L.W. Kang and J.J. Leou, "An error resilient coding scheme for JPEG image transmission based on data embedding and side-match vector quantization," J. Vis. Commun. Image, R.17, pp. 876-891, 2006.
- [5] K.S. Kim, H.Y. Lee, and H.K. Lee, "Supplementary loss concealment technique for image transmission through data hiding," Multimed Tools Appl, vol. 44, pp. 1-16, 2009. (DOI 10.1007/s11042-009-0265-0).
- [6] T.P. Fowdur and K.M.S. Soyjaudah, "Hybrid Joint Source Channel Decoding for Progressive JPEG Image Transmission," Circuits Systems and Signal Processing, vol. 29, pp. 857-879, 2010. (DOI 10.1007/s00034-010-9188-2).
- [7] M. Padmaja, M. Kondaiah and K.S. RamaKrishna, "Error Resilient Image Transmission over Wireless Fading Channels," International Journal of Engineering Science and Technology, vol. 2(5), pp. 1242-1249, 2010.
- [8] A.M. Lakhdar, R.Méliani, and M. Kandouci, "Research on Unequal Error Protection with Punctured Turbo Codes in JPEG Image Transmission System," SJEE, vol.4, no.1, pp. 95-108, June 2007.
- [9] T.P Fowdur and K.M.S Soyjaudah, "Highly Scalable JPEG Image Transmission with Unequal Error Protection and Optimal Feedback," Telecommunication Systems, vol.49, Issue 4, pp. 355-377, 2012. (DOI: 10.1007/s11235-010-9379-y). (Published online: 25 June 2010)
- [10] C.Douillard and C.Berrou, "Turbo codes with Rate-m/(m+1) Constituent Convolutional Codes," in IEEE Trans. Commun, pp. 1630-1638, October 2005.
- [11] J.Vogt and A.Finger, "Improving the MAX-Log-MAP Turbo decoder," Electronics letters, vol. 36, no. 23, November 2000.
- [12] T.Gnanasekaran and K. Duraiswamy, "Performance of Unequal Error Protection Using MAP Algorithm and Modified MAP in AWGN and Fading Channel," Journal of Computer Science, vol. 4 (7), pp. 585-590, 2008.
- [13] B.S. Shim, D.H. Jeong, and S.J. Lim, "A new stopping criterion for turbo codes," in Adv Communication Technology, Ikhсан, pp. 1111-1116, 2006.
- [14] M.R. Soleymani, Y.Gao and U.Vilaipornsawai, Turbo coding for satellite and Wireless Communication, Kluwer Academic Publishers, 2002.
- [15] Y. Ould-Cheikh-Mouhamedou, S. Crozier and P. Kabal, "Distance measurement method for double binary turbo codes and a new interleaver design for DVB-RCS," Global Telecommunications Conference 2004, (GLOBECOM '04), vol. 1, pp. 172 - 178, 2004 .
- [16] Youssouf Ould Cheikh Mouhamedou, On Distance Measurement Methods for Turbo Codes, McGill University, Montreal, PhD Thesis 2005. Available Online: <http://www-mmsp.ece.mcgill.ca/MMSPP/Theses/2005/Ould-Cheikh-MouhamedouT2005.pdf> [Accessed: August 2011]